JOURNAL OF Applied Polymer SCIENCE

Preparation of Thiourea Functionalized Polyvinyl Alcohol-Coated Magnetic Nanoparticles and Their Application in Pb^{2+} Ions Adsorption

Wubin Xiong,[1] Yueping Guan,[1] Chen Guo,[2] Mingzhu Yang,[1] Tingting Xia,[1] Shen Zhao[1]

[1]School of Materials Science and Engineering, University of Science and Technology Beijing, Beijing 100083, China

[2]Laboratory of Separation Science and Engineering, State Key Laboratory of Biochemical Engineering, Institute of Process Engineering, Chinese Academy of Sciences, Beijing 100190, China

Correspondence to: Y. P. Guan (E-mail: ypguan@mater.ustb.edu.cn)

ABSTRACT: We have prepared a novel kind of magnetic nanoparticle with high adsorption capacity and good selectivity for Pb^{2+} ions by modifying the magnetic nanoparticles with polyvinyl alcohol (PVA) and thiourea. The resultant magnetic nanoparticles were used to adsorb Pb^{2+} ions from aqueous solution. The influence of the solution pH, the adsorption time, the adsorption temperature, coexisting ions, and the initial concentration of Pb^{2+} ions on the adsorption of Pb^{2+} ions were investigated. The results indicated that Pb^{2+} ions adsorption was an endothermic reaction, and adsorption equilibrium was achieved within 30 min. The optimal pH for the adsorption of Pb^{2+} ions was pH 5.5, and the maximum adsorption capacity of Pb^{2+} ions was found to be 220 mg/g. Moreover, the coexisting cations such as Ca^{2+}, Co^{2+}, and Ni^{2+} had little effect on adsorption of Pb^{2+} ions. The regeneration studies showed that thiourea functionalized PVA-coated magnetic nanoparticles could be reused for the adsorption of Pb^{2+} ions from aqueous solutions over five cycles without remarkable change in the adsorption capacity. © 2014 Wiley Periodicals, Inc. J. Appl. Polym. Sci. **2014**, *131*, 40777.

KEYWORDS: adsorption; magnetism and magnetic properties; nanoparticles; nanowires and nanocrystals; surfaces and interfaces

Received 4 November 2013; accepted 28 March 2014

DOI: 10.1002/app.40777

INTRODUCTION

Contamination of aquatic media with heavy metals from industrial waste water is a serious environmental problem. Heavy metals are highly toxic at low concentrations and can accumulate in living organisms which cause disorders and diseases.[1] For example, lead is an important compound used as an intermediate in the processing industries such as plating, paint, dyes, and lead batteries; through the food chain system of soil–plant–animal–human, Pb^{2+} ions are transferred into animals and human beings. Lead can directly damage the nervous, reproductive, skeletal systems, and the kidneys, which eventually can even cause cancer.[2] For that reason, more and more researchers pay attention to the separation technology of heavy metals from aqueous solution. The main techniques which have been used on the reduction of metal ions in industrial wastewater are ion exchange,[3,4] chemical precipitation,[5] bio-sorption,[6,7] membrane filtration,[8,9] electrolytic methods,[10] and solvent extraction.[11] However, these methods are limited by the low adsorption rate and capacity, especially at low metal ions concentration.

In recent years, more and more magnetic separation technologies have been applied in the wastewater treatment field for their low energy consumption, less separation steps, and short separation time. Moreover, magnetic separation medium can be reused without remarkable change in the adsorption capacity, and hence results in reducing the cost. There are several reports on applying magnetic separation technology for the removal of organic matter from waste water.[12–18] Magnetic separation technology also has been widely used for solving the problem of heavy metal pollution in water.[19–24] Many researchers modified magnetic nanoparticles by polymer coating the iron oxide.[25,26] The surface modification of magnetic nanoparticles by polymers protects particles from oxidation, and improves dispersability and colloidal stability.[27] The modified magnetic nanoparticles have a good affinity to the metal ions in the wastewater, and the modified magnetic nanoparticles with metal ions can be collected quickly by an external magnetic field. However, the previous reports about the magnetic nanoparticles could not attain a high adsorption capacity and good selectivity toward metal ions in aqueous solution.

Based on the above drawbacks for removal of metal ions, the key factor is that magnetic nanoparticles should have remarkable functional groups on the surface. Moreover, the functional groups of magnetic nanoparticles should have not only high affinity for metal ions but also own selective adsorption capacity for target metal ions. In this article, we modified the magnetic nanoparticles with linear polymer to attain abundant

functional groups on their surface. Then, the polymer-modified magnetic nanoparticles were functionalized with small molecule. Finally, we attained a kind of magnetic nanoparticle with good selectivity and high adsorption capacity for Pb^{2+} ions in aqueous solution.

EXPERIMENTAL

Material

Polyvinyl alcohol (PVA) and sodium hydroxide were purchased from Sinopharm Chemical Reagent Co., Ltd. Epichlorohydrin (ECH) and thiourea were obtained from Tianjin Guangfu Technology Development Co., Ltd. Lead nitrate, calcium nitrate, nickel nitrate, and cobalt nitrate were supplied by Tianjin Guangfu Finechemical Research Institute. Ethylene diamine tetraacetic acid disodium salt was purchased from Xilong Chemical Works Co., Ltd. Ethanol was purchased from Beijing Chemical Works. All reagents are analytical grade. Original magnetic nanoparticles (MNPs-NH_2) which owned amino groups on their surface were obtained from Beijing GiGNano Biointerface Company.

Instrumentation

We used a PHS-25 pH-meter (Shanghai Rex Instrument Factory, China) for pH measurement. Attenuated total reflection-fourier transform infrared spectroscopy (ATR-FTIR) spectra of MNPs-NH_2, PVA-coated magnetic nanoparticles (MNPs-PVA), and thiourea functionalized PVA-coated magnetic nanoparticles (MNPs-Tu) were obtained by an T27-Hyperin-Vector22 IFT-IR (Bruker Corporation, MA) analyzer. Magnetic measurement was carried out using a vibrating sample magnetometer (VSM, 7300, Lakeshore) at 19°C. The dimension and morphology of MNPs-NH_2 were observed by transmission electron microscopy (TEM) (JEM-200CX, FEI, USA). A flame atomic absorption spectrometer (sp-3520(2MT), Shanghai Spectrum Instruments Co. Ltd.) with air–acetylene burner and a single element hollow cathode lamp was used to detect the metal ions concentration. Thermogravimetric analysis was carried out by An Netzsch STA 449C (Netzsch corporation, Bavaria, Germany) analyzer.

Preparation of PVA-Coated Magnetic Nanoparticles

About 100 mL of absolute ethyl alcohol and 30 mL of ECH were dissolved in 100 mL of sodium hydroxide solution of pH 10, and then, a certain amount of MNPs-NH_2 were added into the mixtures by ultrasonic dispersion. The reaction mixtures were kept at 48°C for 6 h under mechanical agitation. After that, the magnetic nanoparticles were separated by a powerful magnet, and washed several times with ethanol and distilled water.

The above prepared magnetic nanoparticles were dispersed in 40 mL of 4% sodium hydroxide solution. Then, the nanoparticle suspension was poured into 200 mL of 5% PVA solution. After 6 h stirring at 80°C, the product was separated by external magnetic field, and washed four times with hot distilled water.

Preparation of Thiourea Functionalized PVA-Coated Magnetic Nanoparticles

MNPs-PVA was added into the mixtures of 90 mL of ethanol and 30 mL of ECH, and then, 90 mL of sodium hydroxide solution of pH 10 were poured into the nanoparticles mixtures. After 6 h stirring at 48°C, the resultant magnetic nanoparticles were separated with a powerful magnet, and washed several times with ethanol and distilled water.

The above magnetic nanoparticles were added into 200 mL of 10% thiourea solution, and then, the nanoparticles suspension solution was adjusted to pH 10 with sodium hydroxide. The mixtures were kept at 80°C for 6 h under mechanical agitation. After that, the MNPs-Tu were collected with a powerful magnet and washed thoroughly with distilled water.

Adsorption Experiments of Pb^{2+} Ions

Adsorption experiments of Pb^{2+} ions were carried out as following operations: (1) mix 15 mg of MNPs-Tu with 20 mL of Pb^{2+} ions solution of different concentrations; (2) adjust the pH value of Pb^{2+} ions solution by standard acid 1*M* HCl and 1*M* NaOH solutions; (3) shake the mixture for 30 min in an orbit shaker operated at 190 rpm. We studied the effect of pH (3.5–5.5), kinetics time (0–100 min), initial concentration of Pb^{2+} ions (100–350 mg/L), and temperature (25°C, 35°C) on adsorption of Pb^{2+} ions in aqueous solution. When the adsorption behavior reached equilibrium, the MNPs-Tu was separated by external magnetic field force. The supernatant of Pb^{2+} ions solution was analyzed by flame atomic absorption spectrometer. The adsorbed amount of Pb^{2+} ions per unit weight of MNPs-Tu was calculated according to the following formula:

$$Q=\frac{(c_0-c)v}{1000M} \quad (1)$$

where Q is the amount of Pb^{2+} ions adsorbed (mg/g), c_0 and c are the initial and final concentration of Pb^{2+} ions (μg/mL), respectively, v is the volume of mixture (mL), M(g) is the amount of MNPs-Tu.

Effect of Coexisting Cations on the Adsorption of Pb^{2+} Ions

The selective adsorption experiment was carried out by a sample containing a mixture of Pb^{2+}, Ca^{2+}, Ni^{2+}, and Co^{2+} ions. The mixture was kept for 30 min at 28°C in an orbit shaker operated at 190 rpm. The concentration of each cation was maintained at 80 mg/L and the pH value is 5.5.

Desorption and Reusability

About 15 mg of MNPs-Tu were added into 20 mL of 80 mg/L Pb^{2+} ions solution. The mixture was kept at 28°C for 30 min and shaken in an orbit shaker operated at 190 rpm. After that, the resultant nanoparticles suspensions were magnetically separated and washed several times with distilled water. We measured the supernatant of residual Pb^{2+} ions solution by flame atomic absorption spectrometer. Then, the ion-loaded magnetic nanoparticles were dispersed in 30 mL of 0.1*M* ETDA and shaken in an orbit shaker operated at 190 rpm for 30 min. We collected the MNPs-Tu by a magnet and washed them with distilled water. The residual solid magnetic nanoparticles were used in above adsorption–desorption cycle experiment for five times.

RESULTS AND DISCUSSION

Modification of Magnetic Nanoparticles

MNPs-Tu were prepared. The reaction pathways are shown in Scheme 1. ECH has been known as a crosslinking agent that

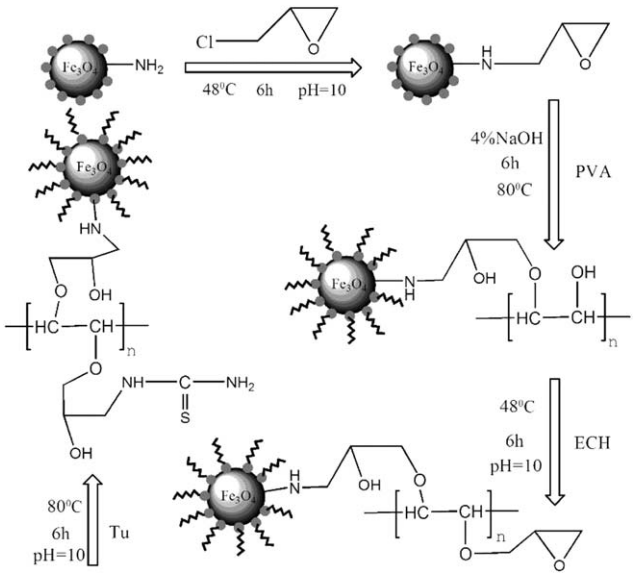

Scheme 1. The reaction pathways of magnetic nanoparticles.

can react with nucleophilic group. The amino groups on the surface of magnetic nanoparticles can replace the chlorine atom in ECH through the nucleophilic reaction and form a carbon amine bond.[28] PVA molecule has remarkable hydroxyl groups in its structure, which can react with the epoxide ring in ECH by the reaction mechanism of nucleophilic attack of atomic oxygen anions which were formed in the alkaline condition.[29,30] The epoxide ring of ECH can easily open when the temperature and alkali are appropriate. Generally, with the increase of temperature and pH value, the epoxide ring-opening reactions become easier. Based on above fact, the chlorine-substitution reaction was given priority to the epoxide ring-opening reactions under 48°C and pH 10. However, if the reaction condition was 80°C and 4% sodium hydroxide solution, the epoxide ring-opening reaction was given priority to the chlorine-substitution reaction. There were a large number of hydroxyl groups on the surface of magnetic nanoparticles after PVA were grafted, which could react with ECH under 48°C and pH 10. Thus, the amino groups in thiourea could attack the epoxy groups by reaction of nucleophilic attack.[31]

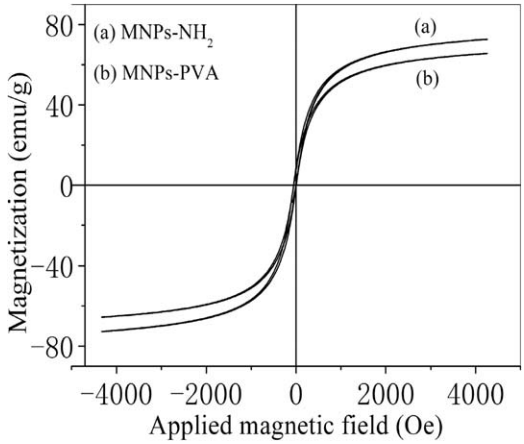

Figure 2. Magnetic hysteresis curves of MNPs-NH_2 (a) and MNPs-PVA (b).

Characterization

TEM. Figure 1 shows the TEM micrograph (a) and normal distribution (b) of MNPs-PVA. As depicted in the picture, the modified magnetic nanoparticles were spherical and had a good dispersibility. The mean diameter was 13 nm, which demonstrated that MNPs-PVA owned a large superficial area.

Magnetization Curve. The magnetic performance of MNPs-PVA and MNPs-NH_2 were measured using VSM at room temperature. Figure 2 shows their typical magnetization loop. It is evident from Figure 2 that MNPs-PVA are superparamagnetic since their coercivity and remanence approaches zero. The saturation magnetization of MNPs-PVA was calculated to be about 65.67 emu/g. Therefore, the MNPs-PVA could be easily separated with the external magnetic field. The saturation magnetization of MNPs-PVA was slightly less than the MNPs-NH_2 (72.72 emu/g), as the MNPs-PVA was oxygenated partly during their preparation.

ATR-FTIR Spectra. In Figure 3(a), the characteristic peak at 3400 cm^{-1} may mean a large number of —OH or N—H on the surface of magnetic nanoparticles. The peaks at 1642 cm^{-1} and 1522 cm^{-1} were the characteristic peak of in-plane bending vibration of primary amine groups. Based on the above data, it could be concluded that there were remarkable amino groups

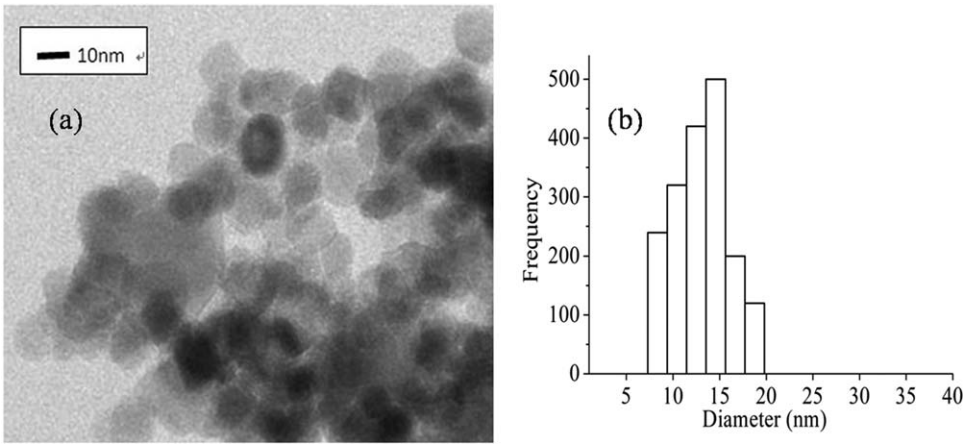

Figure 1. TEM micrograph (a) and size distribution (b) of MNPs-PVA.

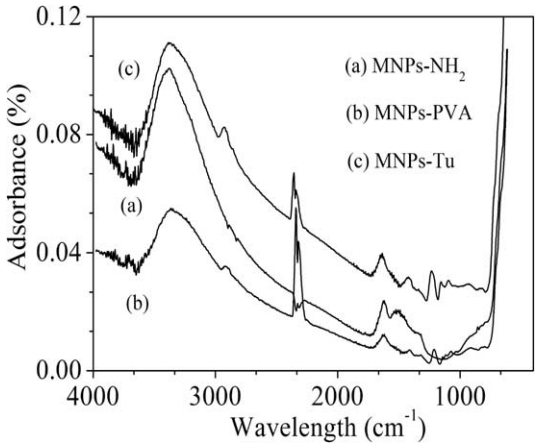

Figure 3. ATR-FTIR spectra of the obtained magnetic nanoparticles: MNPs-NH2 (a), MNPs-PVA (b), and MNPs-Tu (c).

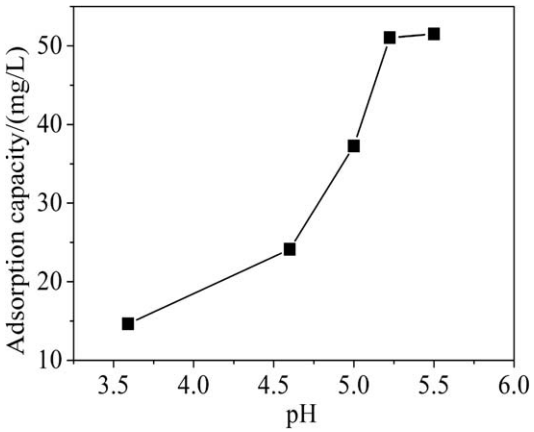

Figure 5. Effect of pH on adsorption of Pb^{2+} ions by MNPs-Tu. (Temperature: 28°C, concentration of Pb^{2+} ions: 80 mg/L).

on the surface of magnetic nanoparticles. As depicted in Figure 3(b), the peak at 2940 cm^{-1} was known to be related to the stretching of C—H, which means remarkable organic groups on the surface of magnetic nanoparticles. The peak at 1233 cm^{-1} was attributed to stretching vibration of C—O—C. The results indicated the presence of PVA on the surface of magnetic nanoparticles as a result of the successful coating procedure. The peak at 1522 cm^{-1} disappeared. It was because the primary amine groups on the nanoparticles did react with the ECH by nucleophilic reaction which made the primary amine turned into tertiary amine. The intensity of the peak at 1233 cm^{-1} and 2940 cm^{-1} in Figure 3(c) became stronger than that in Figure 3(b), which indicated that thiourea might had been modified onto the nanoparticles. Moreover, the stretching vibration peak of N—C at 1410 cm^{-1} in Figure 3(c) became wider than that of Figure 3(b). Based on the above conditions, it suggested that the primary amine groups of thiourea had reacted with the epoxy groups in ECH grafted onto the nanoparticles by nucleophilic mechanism. The two peaks at 2341 cm^{-1} and 2360 cm^{-1} were the characteristic peaks of carbon dioxide.

Thermogravimetric Analysis. TGA thermograms were applied to estimate the amount of the materials modified onto the magnetic nanoparticles. They were heated up to 800°C to ensure the degradation of organic compounds. Figure 4 presents the thermal degradation curves of the MNPs-NH_2 (a) and MNPs-PVA (b). As we can see in Figure 4(a), the MNPs-NH_2 had three weight losses. The residual water from the MNPs-NH_2 was removed when the temperature work up to 100°C. Then, the triethylenetetramine grafted onto the surface of the magnetic nanoparticles were degraded until the temperature reached about 630°C. The weight lose extent of MNPs-NH_2 was 4.07%, which indicated that about 4% triethylenetetramine were modified onto the magnetic nanoparticles. As seen in Figure 4(b), the total weight lose extent was 51%. So we can conclude that there are about 47% PVA having been grafted onto the surface of MNPs-NH_2. Based on above calculation, the productivity of modification for the MNPs-NH_2 was 6.7 $\times$ 10^{-10} mol/m^3. The data showed that modification of MNPs-NH_2 using PVA had been performed successfully.

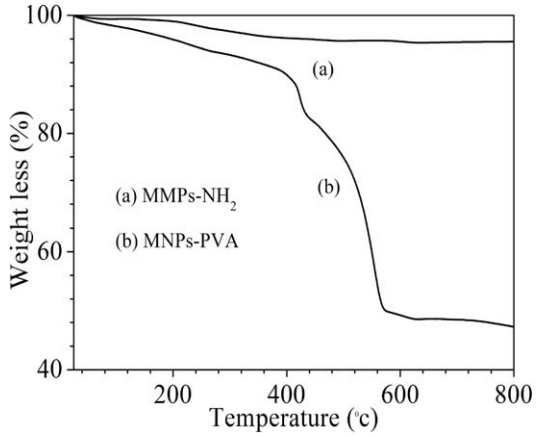

Figure 4. Thermogravimetric analysis of MMPs-NH_2 (a) and MNPs-PVA (b).

Effect of pH on Adsorption of Pb^{2+} Ions

The effect of pH value on the adsorption capacity of MNPs-Tu toward Pb^{2+} ions is shown in Figure 5. The adsorption capacity of MNPs-Tu increased with the increase of pH value. A pH value of 5.5 was not exceeded due to the precipitation of lead hydroxide. It is well known that pH value plays an important role in the adsorption performance of modified magnetic nanoparticles

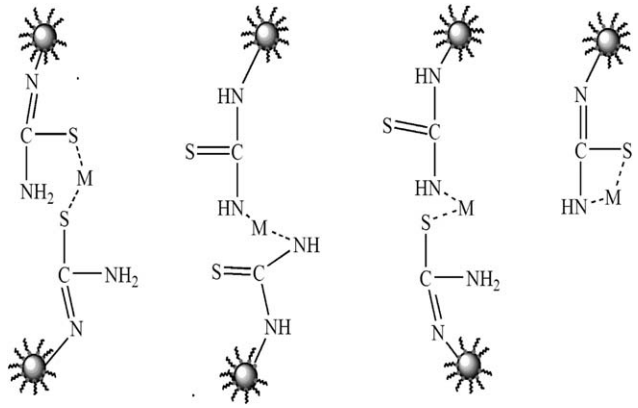

Figure 6. The adsorption mechanism of MNPs-Tu (M represent Pb^{2+} ions, Black ball represent MNPs-Tu).

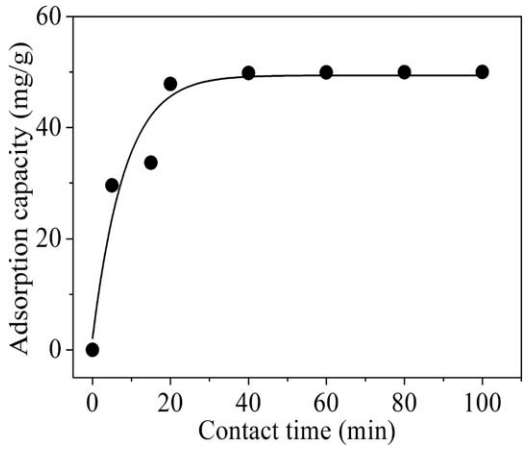

Figure 7. Effect of contact time on MNPs-Tu for the adsorption of Pb^{2+} ions. (Temperature: 28°C, concentration of Pb^{2+} ions: 80 mg/L, pH: 5.5).

toward different heavy metal ions. The pH value of the heavy metal ions solution mainly affects two aspects: heavy metal ions species distribution and the surface charge of magnetic nanoparticles. Because protons of the solution can be adsorbed or released.[32] The change of pH value may be attributed to the change of charge on the surface of MNPs-Tu. With the increase of the pH value of the solution, the surface electronegativity of magnetic nanoparticles with functional groups would increase, which indicates increased electrostatic attraction between nanoparticles and Pb^{2+} ions. The protonation of the functional groups on the surface of magnetic nanoparticles decreased the amount of available functional groups for chelating Pb^{2+} ions when the pH was low. In addition, the positively charged hydronium ions (H_3O^+) competed with the Pb^{2+} ions for binding on the functional groups of the surface on modified magnetic nanoparticles.[33,34] With the increase of pH value, the deprotonation of the functional groups of magnetic nanoparticles would make more available binding sites for complexing Pb^{2+} ions in aqueous solution. Besides that, the electronegative enhancement of MNPs-Tu leads to power electrostatic attraction for receiving the Pb^{2+} ions. The maximum uptake at pH 5.5 may be attributed to the formation of coordination compound between Pb^{2+} ions and deprotonated thiol form of thiourea[35] or deprotonated amino groups. The probable adsorption process is shown in Figure 6.[36]

Adsorption Kinetics

The effect of contact time on the uptake of MNPs-Tu for Pb^{2+} ions is presented in Figure 7. It indicated that the adsorption equilibrium was reached within 30 min, which demonstrated that MNPs-Tu could adsorb rapidly Pb^{2+} ions from aqueous solution.

In order to clarify the mechanism of adsorption kinetics process, several adsorption models were applied to evaluate the experimental data such as pseudo-first-order, pseudo-second-order, and intra-particle diffusion models.

The pseudo-first-order kinetic model can be described as

$$\log(q_e - q_t) = \log q_m - k_1\left(\frac{t}{2.303}\right) \quad (2)$$

where k_1 (min^{-1}) is the pseudo-first-order adsorption rate constant. q_t (mg/g) is the amount of Pb^{2+} ions adsorbed per unit weight of MNPs-Tu at time t (min) q_e (mg/g) signifies the amount of Pb^{2+} ions adsorbed at equilibrium. q_m (mg/g) is the maximum adsorption at equilibrium.

The pseudo-second-order kinetic model is as the following:

$$\frac{t}{q_t} = \frac{1}{k_2 q_e^2} + \frac{1}{q_e}t \quad (3)$$

where k_2 is the pseudo-second-order adsorption rate constant, q_t and q_e are similar to the definition as in eq. (2).

The initial adsorption rate (h) can be calculated from k_2 and q_e values[37] using:

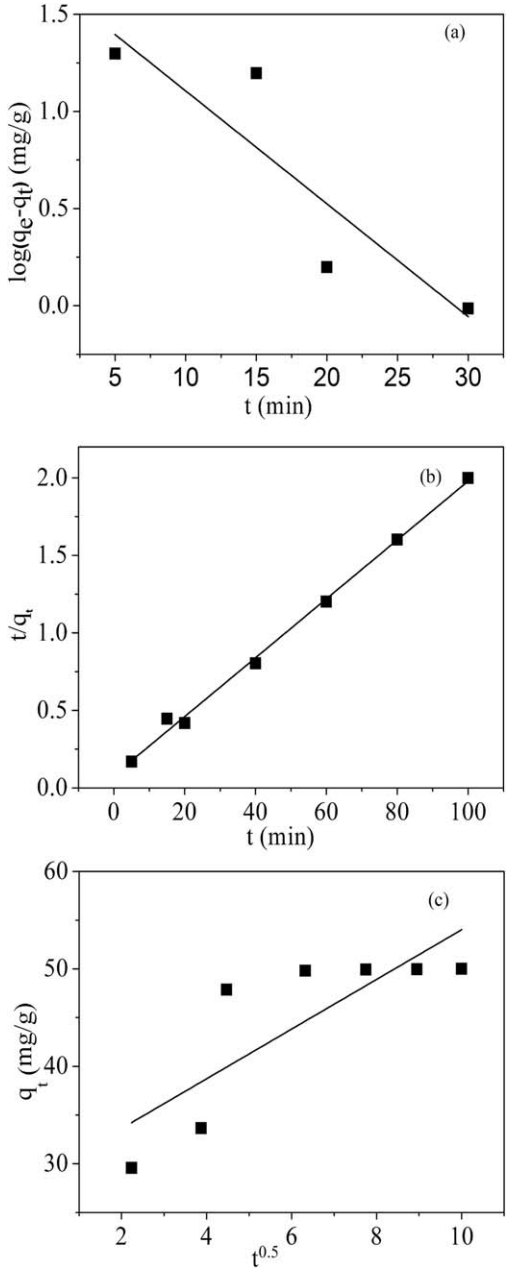

Figure 8. Adsorption kinetics of MNPs-Tu for the adsorption of Pb^{2+} ions: pseudo-first-order kinetic model (a); pseudo-second-order kinetic model (b); intra-particle diffusion model (c).

Table I. Kinetic Parameters of Pb^{2+} Ions Adsorption by MNPs-Tu

First-order model			Second-order model				Inter-particle model	
K_1 (min^{-1})	q_1 (mg/g)	R^2	K_2 (g/(mg min))	q_2 (mg/g)	h (mg/(g min))	R^2	K (mg/(g $min^{1/2}$))	R^2
0.1338	48.59147	0.8060	4.49×10^{-3}	52.65929	12.45	0.9962	2.55	0.6709

$$h = k_2 q_e^2 \quad (4)$$

The linear form of the intra-particle diffusion model equation is:

Intra-particle diffusion equation:

$$q_t = kt^{0.5} + I \quad (5)$$

k(mg/g min^{-1}) is the intra-particle diffusion rate constant and I(mg/g) is a constant that provides information on the thickness of the boundary layer.

The validities of these three kinetic models are described in Figure 8. And the values of the correlation coefficients and the parameters calculated from these three models are all listed in Table I. The R^2 value for the pseudo-second-order model was greater than other kinetic model, reaching 0.9962. Moreover, the maximum adsorption value (q_e) calculated from the pseudo-second-order kinetic model was 52.66 mg/g, which was close to the experimental value. According to the results, the pseudo-second-order model was best fit for the experimental kinetic data. Thus, the rate-limiting step may be the chemical adsorption.[38] The initial adsorption rate of MNPs-Tu was 12.45 mg/(g min), which was fast and controlled by diffusion. Then, the Pb^{2+} ions of solution engaged with chelating exchanger reaction were slower and controlled by a second-order chemical reaction. It can be explained that there were abundant amine and sulfur groups on the MNPs-Tu. These amine and sulfur sites are the main reactive groups for Pb^{2+} ion to bind through chelation reaction.

Adsorption Isotherms

The effect of initial Pb^{2+} ions concentration on the MNPs-Tu for adsorption of Pb^{2+} ions at different temperature is shown in Figure 9. The results of the experiment indicated that the equilibrium adsorption capacity of Pb^{2+} ions increased with the increase of the initial Pb^{2+} ions concentration. The adsorption capacity increased with increase of the temperature, which demonstrated that the adsorption reaction was endothermic. It may be because that the heavy metal ions were well hydrated, and they had to lose part of hydration sheath to be adsorbed onto the MNPs-Tu. This dehydration process of heavy metal ions need to receive energy and superseded the exothermicity of the heavy metal ions adsorbed on the surface.[39] We could obtain the maximum adsorption capacity of MNPs-Tu for Pb^{2+} ions when the initial Pb^{2+} ions concentration is 350 mg/g at different temperature. It could be explained that the chelation interaction between the MNPs-Tu and Pb^{2+} ions were easier when the initial Pb^{2+} ions concentration increased. Moreover, the Pb^{2+} ions could diffuse onto the surface of MNPs-Tu at a higher rate as temperature of the Pb^{2+} ions solution and the initial Pb^{2+} ions concentration rises.[40] The comparison of the maximum Pb^{2+} ions adsorption capacity of MNPs-Tu obtained in this work and with other results reported in literatures is shown in Table II. As we can see in the table, the adsorption capacity of MNPs-Tu in the work was comparatively higher than other adsorbents.

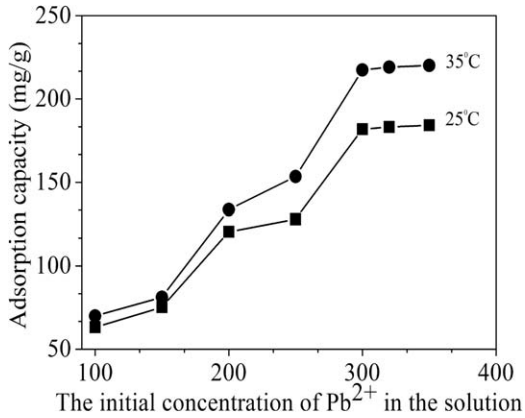

Figure 9. Equilibrium adsorption isotherms of Pb^{2+} ions by MNPs-Tu. (pH: 5.5).

Several isotherm models were used to clarify the adsorption data such as Langmuir isotherm models and Freundlich isotherm models. The R^2 value of Langmuir isotherm models were 0.2156 (25°C) and 0.12156 (35°C), respectively, which were of no worth for evaluating the adsorption capacity. So we only analyzed the data using Freundlich isotherm models.

The Freundlich isotherm models can be described as:

$$\mathrm{Ln}q_e = \mathrm{Ln}k + \frac{1}{n}\mathrm{Ln}c_e \quad (6)$$

where both k and n are Freundlich constants, which express adsorption capacity and adsorption intensity, respectively, where

Table II. Maximum Adsorption Capacity of Pb^{2+} Ions Onto Various Adsorbents

Adsorbents	Maximum adsorption capacity (mg/g)	References
Iron oxide	36	[41]
Nanoparticles		
Magnetic carbonaceous	123.1	[42]
Nanoparticles		
Blast furnace sludge	64.17	[43]
Pterygota macrocarpa sawdust	115.61	[44]
Graphene oxide	80.775	[45]
Tea waste	65	[46]
Activated carbon	26.5	[47]
MNPs-Tu	220	this study

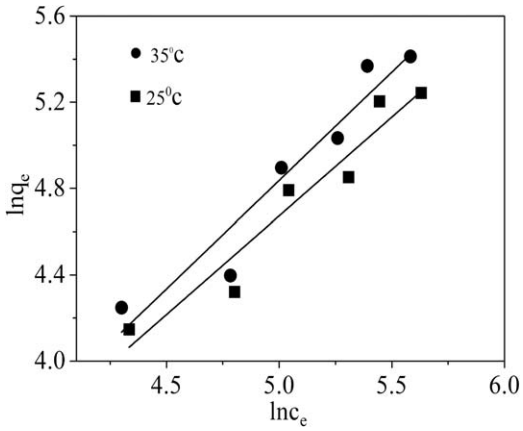

Figure 10. Adsorption isotherms of MNPs-Tu for Pb^{2+} ions at different temperature.

Table III. Freundlich Isothermal Parameters of Pb^{2+} Ions Adsorption by MNPs-Tu

Temperature (°C)	*n*	*k*	R^2
25	1.093	1.1036	0.96556
35	0.9949	0.8285	0.96198

q_e (mg/g) is the amount of Pb^{2+} ions adsorbed onto the MNPs-Tu at equilibrium, c_e (mg/L) stand for the equilibrium Pb^{2+} ions concentration of the solution.

The linear adsorption isotherms of Freundlich models at different temperature are shown in Figure 10. The parameters and correlation coefficients from the kinetic models are all listed in Table III. The R^2 value for Freundlich isotherm models was greater than the one for Langmuir isotherm models, which indicated that Freundlich isotherm models may better fit to the experimental data. Moreover, the *n*values at different temperature were between 1 and 10, representing beneficial adsorption. Thus, we may conclude that the Pb^{2+} ions in the solution were adsorbed onto the surface of MNPs-Tu in a multilayer adsorption form[48] and the adsorption of the surface of MNPs-Tu were heterogeneous.[49]

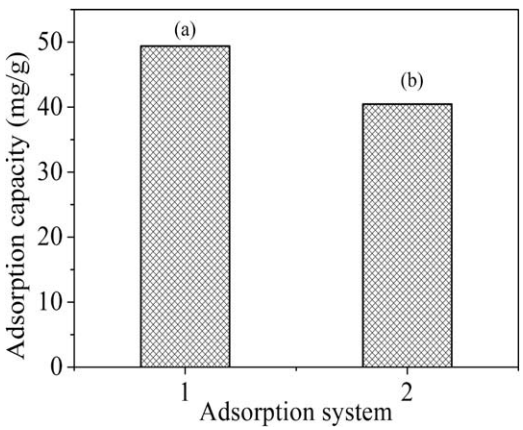

Figure 11. Effect of coexisting cations on the adsorption of Pb^{2+} ions: (a) unitary system, (b) multicomponent system.

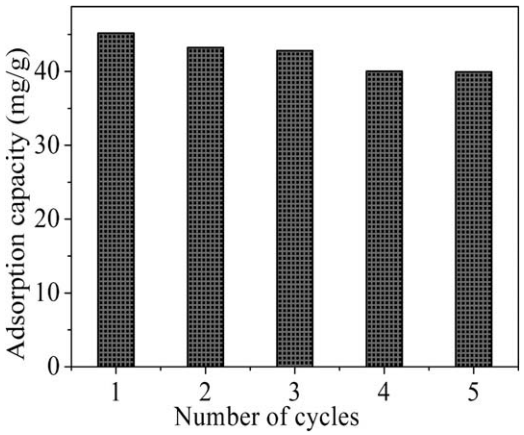

Figure 12. Reusability of MNPs-Tu for adsorption/desorption of Pb^{2+} ions during five cycles. (Temperature: 28°C, pH: 5.5, concentration of Pb^{2+}: 80 mg/L. Desorption: concentration of ETDA: 0.1 mol/L).

Effect of Coexisting Cations on the Adsorption of Pb^{2+} Ions

As we know, the other cations in the industry water may create unfavorable effect on adsorption of target metal ions. Thus, the effect of coexisting cations (Ca^{2+}, Ni^{2+}, and Co^{2+}) on the adsorption capacity of MNPs-Tu toward Pb^{2+} ions were investigated. The results are shown in Figure 11. As seen in the picture, the adsorption capacity was 40.456 mg/g after the selective experiment, which decreased 18.09% compared with the single Pb2+ ions system. It could be explained that some of the Ca^{2+}, Ni^{2+}, and Co^{2+} ions were collected by the MNPs-Tu. Because the molecular mass, ion charges, and hydration energy of the metal ions can influence their interaction with modified magnetic nanoparticles.[50] The results of the experiment indicated that coexisting cations had no noteworthy influence on the adsorption of Pb^{2+} ions. Thus, it indicated that MNPs-Tu could selectively adsorb Pb^{2+} ions in aqueous solution.

Reuse of Thiourea Functionalized PVA-Coated Magnetic Nanoparticles

For potential practical applications, the regeneration and reuse of an adsorbent are important. The Pb^{2+} ions adsorbed onto the MNPs-Tu were released using 30 mL of 0.1*M* EDTA solution. In order to show the reusability of MNPs-Tu, the adsorption–desorption cycle experiment of Pb^{2+} ions were repeated five times using the same nanoparticles. The results of the cyclic test are shown in Figure 12. The adsorption capacity did not change significantly during the cyclic test, which indicated that MNPs-Tu own a well reusability. It could be explained that lead ions adsorbed by MNPs-Tu were not desorbed completely. These lead ions occupied the adsorption area of MNPs-Tu, which led to the change of adsorption capacity.

CONCLUSIONS

Magnetic nanoparticles modified with PVA and thiourea can adsorb Pb^{2+} ions in aqueous solution in a short time. The adsorption capacity of MNPs-Tu strongly depends on the pH value. The best pH condition for the adsorption of Pb^{2+} ions is pH 5.5. The adsorption capacity of MNPs-Tu increases with the increase of initial concentration of Pb^{2+} ions, and the maximum

adsorption capacity can reach 220 mg/g. The MNPs-Tu can adsorb further quantity of Pb^{2+} ions from the aqueous solution when the temperature of the solution becomes higher. Coexisting ions have little influence on the adsorption capacity of Pb^{2+} ions. The MNPs-Tu has good durability as well as good efficiency for repeated use. Adsorption kinetics of the MNPs-Tu is better fit to the pseudo-second-order model by fitting the data, which demonstrated that the rate-limiting step may be the chemical adsorption. Adsorption isotherms of the MNPs-Tu based on the data of different initial concentration of Pb^{2+} ions in the solution are agreed with the Freundlich isotherm model, which indicated the surface of MNPs-Tu is heterogeneous and multilayer adsorption.

ACKNOWLEDGMENTS

This work was financially supported by National Natural Science Foundation of China (51274035) and National Basic Research Program of China (2013CB632602).

REFERENCES

1. Meena, A. K.; Mishra, G. K.; Rai, P. K.; Rajagopal, C.; Nagar, P. N. *J. Hazard. Mater.* **2005**, *122*, 161.
2. Xu, M.; Zhang, Y. S.; Zhang, Z. M.; Shen, Y. U.; Zhao, M. J.; Pan, G. T. *Chem. Eng. J.* **2011**, *168*, 737.
3. Pansini, M.; Colella, C.; Gennaro, M. D. *Desalination* **1991**, *83*, 145.
4. Taty-Costodes, V. C.; Fauduet, H.; Porte, C.; Delacroix, A. *J. Hazard. Mater.* **2003**, *105*, 121.
5. Charerntanyarak, L. *Water Sci. Technol.* **1999**, *39*, 135.
6. Marques, P.; Rosa, M. F.; Pinheiro, H. M. *Bioprocess. Eng.* **2000**, *23*, 135.
7. Shao, W. J.; Chen, L. H.; Lü, L. L.; Luo, F. *Desalination* **2011**, *265*, 177.
8. Juang, R. S.; Shiau, R.C. *J. Membr. Sci.* **2000**, *165*, 159.
9. Ahn, K. H.; Song, K. G.; Cha, H. Y.; Yeom, I. T. *Desalination* **1999**, *122*, 77.
10. Janssen, L. J. J.; Koene, L. *Chem. Eng. J.* **2002**, *85*, 137.
11. Yun, C. H.; Prasad, R.; Guha, A. K.; Sirkar K. K. *Ind. Eng. Chem. Res.* **1993**, *32*, 1186.
12. Afkhami, A.; Moosavi, R. *J. Hazard. Mater.* **2010**, *174*, 398.
13. Zhang, W.; Liang, F.; Li, C.; Qiu, L. G.; Yuan, Y. P.; Peng, F. M.; Jiang, X.; Xie, A. J.; Shen, Y. H.; Zhu, J. F. *J. Hazard. Mater.* **2011**, *186*, 984.
14. Singha, K. P.; Guptaa, S.; Singha, A. K.; Sinha, S. *J. Hazard. Mater.* **2011**, *186*, 1462.
15. Borghi, C. C.; Fabbri, M.; Fiorini, M.; Mancini, M.; Ribani, P. L. *Sep. Purif. Technol.* **2011**, *83*, 180.
16. Gad-Allah, T. A.; Kato, S.; Satokawa, S.; Kojima, T. *Desalination* **2009**, *244*, 1.
17. Rochera, V.; Beea, A.; Siauguea, J. M.; Cabuil, V. *J. Hazard. Mater.* **2010**, *178*, 434.
18. Ying, C.; Umetsu, K.; Ihara, I.; Sakai, Y.; Yamashiro, T. *Bioresour. Technol.* **2010**, *101*, 4349.
19. Wang, Q.; Guan, Y. P.; Ren, X. F.; Yang, M. Z.; Liu X. *Chem. Eng. J.* **2012**, *183*, 339.
20. Wang, Q.; Guan, Y. P.; Ren, X. F.; Yang, M. Z.; Liu X. *Colloid Interface Sci.* **2012**, *374*, 325.
21. Wei, L. S.; Yang, G.; Wang, R.; Ma, W. *J. Hazard. Mater.* **2009**, *164*, 1159.
22. Badruddoza, A. Z. M.; Tay, A. S. H.; Tan, P. Y.; Hidajat, K.; Uddin, M. S. *J. Hazard. Mater.* **2011**, *185*, 1177.
23. Zhua, Y. H.; Hua, J.; Wang, J. L. *J. Hazard. Mater.* **2012**, *221–222*, 155.
24. Chaabouni, A.; Marzougui, Z.; Elleuch, B.; Eissa, M. M.; Elaissari, A. *Sci. Adv. Mater.* **2013**, *5*, 854.
25. Ahmad, H. J. *Colloid Sci. Biotechnol* **2013**, *2*, 155.
26. Medeiros, S. F.; Lara, B. R.; Oliveira, P. F. M.; Moraes, R. M.; Alves, G. M.; Elaissari, A.; Santos, A. M. *J. Colloid Sci. Biotechnol.* **2013**, *2*, 180.
27. Rahman, M. M.; Elaissari, A. *Adv. Polym. Sci.* **2010**, *233*, 237.
28. Zhou, L. M.; Liu, Z. R.; Liu, J. H.; Huang, Q. W. *Desalination* **2010**, *258*, 41.
29. Kim, D. H.; Na, S. K.; Park, J. S.; Yoon, K. J. *Eur. Polym. J.* **2002**, *38*, 1199.
30. Das, K.; Ray, D.; Bandyopadhyay, N. R.; Gupta, A.; Sengupta, S.; Sahoo, S.; Mohanty, A.; Misra, M. *Ind. Eng. Chem. Res.* **2010**, *49*, 2176.
31. Zhou, L. M.; Wang, Y. P.; Liu, Z. R.; Huang, Q. W. *J. Hazard. Mater.* **2009**, *161*, 995.
32. Ou, Q. Q.; Zhou, L.; Zhao, S. G.; Geng, H. J.; Hao, J. J.; Xu, Y. Y.; Chen, H. L. *Chem. Eng. J.* **2012**, *180*, 121.
33. Xu, M.; Zhang, Y. S.; Zhang, Z. M.; Shen, Y. O.; Zhao, M. J.; Pan, G. T. *Chem. Eng. J.* **2011**, *168*, 737.
34. Chen, A. W.; Zeng, G. M.; Chen, G. Q.; Hu, X. J.; Yan, M.; Guan, S.; Shang, C.; Lu, L. H.; Zou, Z. J.; Xie, G. X. *Chem. Eng. J.* **2012**, *191*, 85.
35. Donia, A. M.; Atia, A. A.; Heniesh, A. M. *Sep. Purif. Technol.* **2008**, *60*, 46.
36. Dey, R. K.; Oliveira, A. S.; Patnaik, T.; Singh, V. K.; Tiwary, D.; Airoldi, C. *J. Solid State Chem.* **2009**, *182*, 2010.
37. Ho, Y. S.; McKay, G. *Water Res.* **2000**, *34*, 735.
38. Yurdakoc, M.; Scki, Y.; Yuedakoc, S. K. *J. Colloid Interface Sci.* **2005**, *286*, 440.
39. Naseem, R.; Tahir, S. S. *Water Res.* **2001**, *35*, 3982.
40. Kannamba, B.; Laxma Reddy, K.; Appa Rao, B. V. *J. Hazard. Mater.* **2010**, *175*, 939.
41. Nassar, N. N. *J. Hazard. Mater.* **2010**, *184*, 538.
42. Nata, I. F.; Salim, G. W.; Lee, C. K. *J. Hazard. Mater.* **2010**, *183*, 853.
43. Lopez, D. A.; Perez, C.; Lopez, F. A. *Water Res.* **1998**, *32*, 989.
44. Adouby, K.; Akissi, L. C. K.; Wandan, N. E.; Yao, B. *J. Appl. Sci.* **2007**, *14*, 1864.
45. Liu, L.; Liu, S. X.; Zhang, Q. P.; Li, C.; Bao, C. L.; Liu, X. T.; Xiao, P. F. *J. Chem. Eng. Data* **2013**, *58*, 209.
46. Amarasinghe, B.; Williams, R. A. *Chem. Eng. J.* **2007**, *132*, 299.

47. Sekar, M.; Sakthi, V.; Rengaraj, S. *J. Colloid Interface Sci.* **2004**, *279*, 307.
48. Ruparelia, J. P.; Duttagupta, S. P.; Chatterjee, A. K.; Mukherji, S. *Desalination* **2008**, *232*, 145.
49. Wang, L. X.; Li, J. C.; Jiang, Q.; Zhao, L. J. *Dalton Trans.* **2012**, *41*, 4544.
50. Lv, L.; Hor, M. P.; Su, F.; Zhao, X. S. *J. Colloid Interface Sci.* **2005**, *287*, 178.